LETTER

doi:10.1038/nature15759

Loophole-free Bell inequality violation using electron spins separated by 1.3 kilometres

B. Hensen[1,2], H. Bernien[1,2]†, A. E. Dréau[1,2], A. Reiserer[1,2], N. Kalb[1,2], M. S. Blok[1,2], J. Ruitenberg[1,2], R. F. L. Vermeulen[1,2], R. N. Schouten[1,2], C. Abellán[3], W. Amaya[3], V. Pruneri[3,4], M. W. Mitchell[3,4], M. Markham[5], D. J. Twitchen[5], D. Elkouss[1], S. Wehner[1], T. H. Taminiau[1,2] & R. Hanson[1,2]

More than 50 years ago[1], John Bell proved that no theory of nature that obeys locality and realism[2] can reproduce all the predictions of quantum theory: in any local-realist theory, the correlations between outcomes of measurements on distant particles satisfy an inequality that can be violated if the particles are entangled. Numerous Bell inequality tests have been reported[3–13]; however, all experiments reported so far required additional assumptions to obtain a contradiction with local realism, resulting in 'loopholes'[13–16]. Here we report a Bell experiment that is free of any such additional assumption and thus directly tests the principles underlying Bell's inequality. We use an event-ready scheme[17–19] that enables the generation of robust entanglement between distant electron spins (estimated state fidelity of 0.92 ± 0.03). Efficient spin read-out avoids the fair-sampling assumption (detection loophole[14,15]), while the use of fast random-basis selection and spin read-out combined with a spatial separation of 1.3 kilometres ensure the required locality conditions[13]. We performed 245 trials that tested the CHSH–Bell inequality[20] $S \leq 2$ and found $S = 2.42 \pm 0.20$ (where S quantifies the correlation between measurement outcomes). A null-hypothesis test yields a probability of at most $P = 0.039$ that a local-realist model for space-like separated sites could produce data with a violation at least as large as we observe, even when allowing for memory[16,21] in the devices. Our data hence imply statistically significant rejection of the local-realist null hypothesis. This conclusion may be further consolidated in future experiments; for instance, reaching a value of $P = 0.001$ would require approximately 700 trials for an observed $S = 2.4$. With improvements, our experiment could be used for testing less-conventional theories, and for implementing device-independent quantum-secure communication[22] and randomness certification[23,24].

We consider a Bell test in the form proposed by Clauser, Horne, Shimony and Holt (CHSH)[20] (Fig. 1a). The test involves two boxes labelled A and B. Each box accepts a binary input (0 or 1) and subsequently delivers a binary output (+1 or −1). In each trial of the Bell test, a random input bit is generated on each side and input to the respective box. The random input bit triggers the box to produce an output value that is recorded. The test concerns correlations between the output values (labelled x and y for boxes A and B, respectively) and the input bits (labelled a and b for A and B, respectively) generated within the same trial.

The discovery made by Bell is that in any theory of physics that is both local (physical influences do not propagate faster than light) and realistic (physical properties are defined before, and independent of, observation) these correlations are bounded more strongly than they are in quantum theory. In particular, if the input bits can be considered free random variables (condition of 'free will') and the boxes are sufficiently separated such that locality prevents communication between the boxes during a trial, then the following inequality holds under local realism:

$$S = \left| \langle x \cdot y \rangle_{(0,0)} + \langle x \cdot y \rangle_{(0,1)} + \langle x \cdot y \rangle_{(1,0)} - \langle x \cdot y \rangle_{(1,1)} \right| \leq 2 \qquad (1)$$

where $\langle x \cdot y \rangle_{(a,b)}$ denotes the expectation value of the product of x and y for input bits a and b. (A mathematical formulation of the concepts underlying Bell's inequality is found in, for example, ref. 25.)

Quantum theory predicts that the Bell inequality can be significantly violated in the following setting. We add one particle, for example an electron, to each box. The spin degree of freedom of the electron forms a two-level system with eigenstates $|\uparrow\rangle$ and $|\downarrow\rangle$. For each trial, the two spins are prepared into the entangled state $|\psi^-\rangle = (|\uparrow\downarrow\rangle - |\downarrow\uparrow\rangle)/\sqrt{2}$. The spin in box A is then measured along direction Z (for input bit $a = 0$) or X (for $a = 1$) and the spin in box B is measured along $(-Z+X)/\sqrt{2}$ (for $b = 0$) or $(-Z-X)/\sqrt{2}$ (for $b = 1$). If the measurement outcomes are used as outputs of the boxes, then quantum theory predicts a value of $S = 2\sqrt{2}$, which shows that the combination of locality and realism is fundamentally incompatible with the predictions of quantum mechanics.

Bell's inequality provides a powerful recipe for probing fundamental properties of nature: all local-realist theories that specify where and when the free random input bits and the output values are generated can be experimentally tested against it.

Violating Bell's inequality with entangled particles poses two main challenges: excluding any possible communication between the boxes (locality loophole[13]) and guaranteeing efficient measurements (detection loophole[14,15]). First, if communication is possible, a box can in principle respond using knowledge of both input settings, rendering the Bell inequality invalid. The locality conditions thus require boxes A and B and their respective free-input-bit generations to be separated in such a way that signals travelling at the speed of light (the maximum allowed under special relativity) cannot communicate the local input setting of box A to box B, before the output value of box B has been recorded, and vice versa. Second, disregarding trials in which a box does not produce an output bit (that is, assuming fair sampling) would allow the boxes to select trials on the basis of the input setting. The fair sampling assumption thus opens a detection loophole[14,15]: the selected subset of trials may show a violation even though the set of all trials may not.

The locality loophole has been addressed with pairs of photons separated over a large enough distance, in combination with fast settings changes[4] and later with settings determined by fast random number generators[5,9]. However, these experiments left open the detection loophole, owing to imperfect detectors and inevitable photon loss during the spatial distribution of entanglement. The detection loophole has been closed in different experiments[6–8,10–12], but these did not

[1]QuTech, Delft University of Technology, PO Box 5046, 2600 GA Delft, The Netherlands. [2]Kavli Institute of Nanoscience Delft, Delft University of Technology, PO Box 5046, 2600 GA Delft, The Netherlands. [3]ICFO-Institut de Ciencies Fotoniques, The Barcelona Institute of Science and Technology, 08860 Castelldefels (Barcelona), Spain. [4]ICREA-Institució Catalana de Recerca i Estudis Avançats, Lluis Companys 23, 08010 Barcelona, Spain. [5]Element Six Innovation, Fermi Avenue, Harwell Oxford, Didcot, Oxfordshire OX11 0QR, UK. †Present address: Department of Physics, Harvard University, Cambridge, Massachusetts 02138, USA.

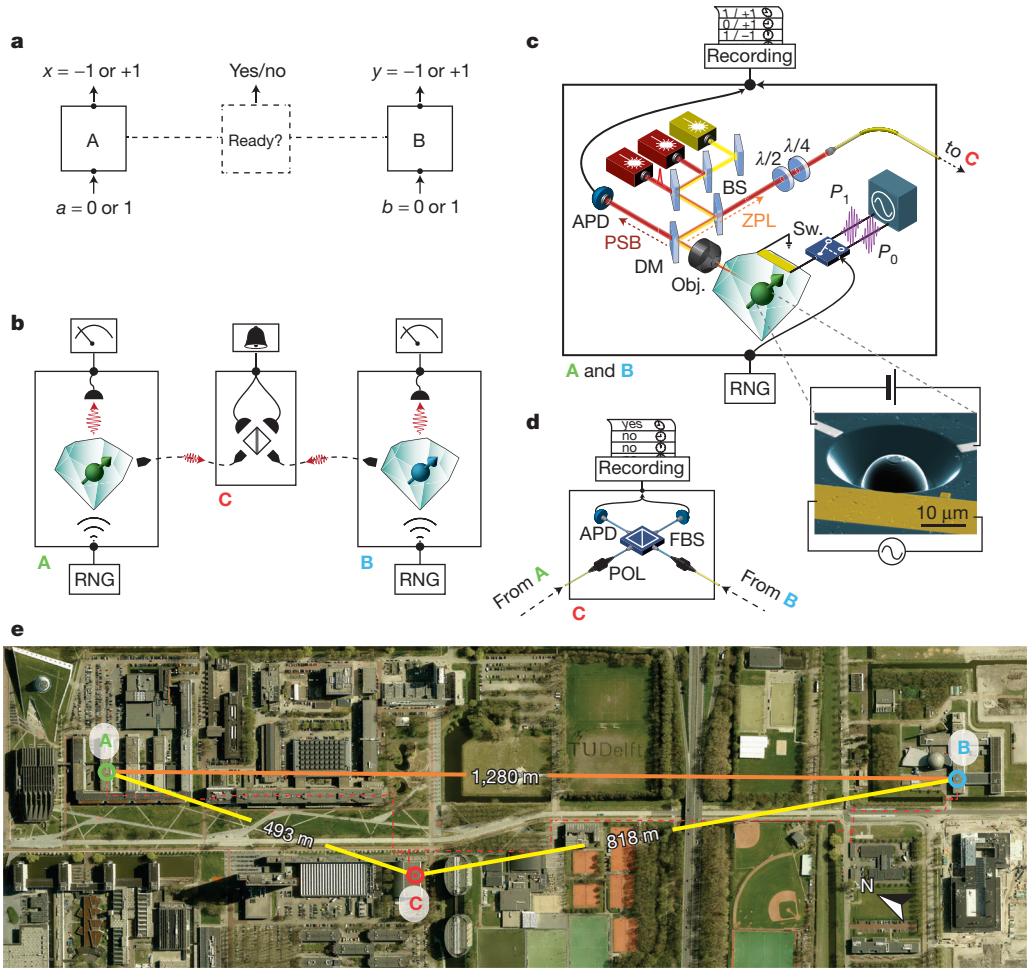

Figure 1 | Bell-test schematic and experimental realization. **a**, Bell-test set-up: two boxes, A and B, accept binary inputs (a, b) and produce binary outputs (x, y). In an event-ready scenario, an additional box C gives a binary output signalling that A and B were successfully prepared. **b**, Experimental realization. The set-up consists of three separate laboratories, A, B and C. The boxes at locations A and B each contain a single NV centre in diamond. A quantum random-number generator (RNG) is used to provide the input. The NV electronic spin is read out in a basis that depends on the input bit, and the resultant signal provides the output. A box at location C records the arrival of single photons that were previously emitted by, and entangled with, the spins at A and B. **c**, Experimental set-up at A and B. The NV centre is located in a low-temperature confocal microscope (Obj.). Depending on the output of the RNG, a fast switch (Sw.) transmits one of two different microwave pulses (P_0 and P_1) into a gold line deposited on the diamond surface (inset, scanning electron microscope image). Pulsed red and yellow lasers are used to resonantly excite the optical transitions of the NV centre. The emission (dashed arrows) is spectrally separated into an off-resonant part (phonon side band, PSB) and a resonant part (zero-phonon line, ZPL), using a dichroic mirror (DM). The PSB emission is detected with a single-photon counter (APD). The ZPL emission is transmitted through a beam-sampler (BS, reflection $\leq$4%) and wave plates ($\lambda/2$ and $\lambda/4$), and sent to location C through a single-mode fibre. **d**, Set-up at location C. The fibres from A and B are connected to a fibre-based beam splitter (FBS) after passing a fibre-based polarizer (POL). Photons in the output ports are detected and recorded. **e**, Aerial photograph of the campus of Delft University of Technology indicating the distances between locations A, B and C. The red dotted line marks the path of the fibre connection. Aerial photograph by Slagboom en Peeters Luchtfotografie BV.

close the locality loophole. So far, no experiment has closed all the loopholes simultaneously.

A Bell test that closes all experimental loopholes at the same time—commonly referred to as a loophole-free Bell test[15,19]—is of foundational importance to the understanding of nature. In addition, a loophole-free Bell test is a critical component for device-independent quantum security protocols[22] and randomness certification[23,24]. In such adversarial scenarios, all loopholes are ideally closed because they allow for security breaches in the system[26].

One approach for realizing a loophole-free set-up was proposed by Bell himself[17]. The key idea is to record an additional signal (dashed box in Fig. 1a) to indicate whether the required entangled state was successfully shared between A and B, that is, whether the boxes were ready to be used for a trial of the Bell test. By conditioning the validity of a Bell-test trial on this event-ready signal, failed entanglement distribution events are excluded upfront from being used in the Bell test.

We implemented an event-ready Bell set-up[18,19] with boxes that use the electronic spin associated with a single nitrogen-vacancy (NV) defect centre in a diamond chip (Fig. 1b). The diamond chips are mounted in closed-cycle cryostats ($T = 4$ K) located in distant laboratories named A and B (Fig. 1c). We control the electronic spin state of each NV centre with microwave pulses applied to on-chip striplines (Fig. 1c, inset). The spins are initialized through optical pumping and read out along the Z axis via spin-dependent fluorescence[27]. The read-out relies on resonant excitation of a spin-selective cycling transition (12-ns lifetime), which causes the NV centre to emit many photons when it is in the bright $m_s = 0$ spin state, while it remains dark when it is in either of the $m_s = \pm 1$ states. We assign the value $+1$ ($m_s = 0$) to the output if we record at least one photo-detector count during the read-out window, and the value -1 ($m_s = \pm 1$) otherwise. Read-out in a rotated basis is achieved by first rotating the spin, followed by read-out along Z.

We generate entanglement between the two distant spins by entanglement swapping[18] in the Barrett–Kok scheme[28,29] using a third loca-

tion C (roughly midway between A and B; see Fig. 1e). First we entangle each spin with the emission time of a single photon (time-bin encoding). The two photons are then sent to location C, where they are overlapped on a beam-splitter and subsequently detected. If the photons are indistinguishable in all degrees of freedom, then the observation of one early and one late photon in different output ports projects the spins at A and B into the maximally entangled state $|\psi^-\rangle = (|\uparrow\downarrow\rangle - |\downarrow\uparrow\rangle)/\sqrt{2}$, where $m_s = 0 \equiv |\uparrow\rangle$ and $m_s = -1 \equiv |\downarrow\rangle$. These detections herald the successful preparation and play the role of the event-ready signal in Bell's proposed set-up. As can be seen in the space–time diagram in Fig. 2a, we ensure that this event-ready signal is space-like separated from the random input-bit generation at locations A and B.

The separation of the spins by 1,280 m defines a 4.27-μs time window during which the local events at A and B are space-like separated from each other (see the space–time diagram in Fig. 2b). To comply with the locality conditions of the Bell test, the choice of measurement bases and the measurement of the spins should be performed within this time window. For the basis choice we use fast random-number generators with real-time randomness extraction[30]. We reserve 160 ns for the random basis choice, during which time one extremely random bit is generated from 32 partially random raw bits (Supplementary Information). The random bit sets the state of a fast microwave switch that selects one out of two preprogrammed microwave pulses implementing the two possible read-out bases (Fig. 1c). Adding the durations of each of the above steps yields a maximum time from the start of the basis choice to the start of the read-out of 480 ns. We choose the read-out duration to be 3.7 μs, which leaves 90 ns to cover any uncertainty in the distance between the laboratories and the synchronization of the set-up (estimated total error is at most 16 ns; see Supplementary Information). For this read-out duration, the combined initialization and single-shot read-out fidelity of sample A is (97.1 ± 0.2)% (Fig. 2c); sample B achieves (96.3 ± 0.3)%. In summary, the use of the event-ready scheme enables us to comply with the strict locality conditions of the Bell set-up by using photons to distribute entanglement, while simultaneously using the single-shot nature of the spin read-out to close the detection loophole.

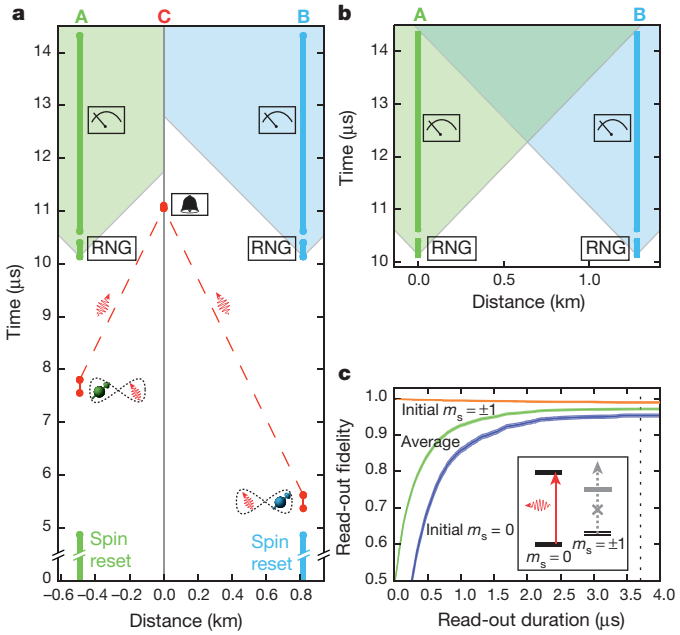

Figure 2 | Space–time analysis of the experiment. **a**, Space–time diagram of a single repetition of the entanglement generation. The *x* axis denotes the distance along the lines AC and CB. After spin initialization, spin-photon entanglement is generated, such that the two photons from A and B arrive simultaneously at C where the detection time of the photons is recorded. Successful preparation of the spins is signalled (bell symbol) by a specific coincidence detection pattern. Independent of the event-ready signal, the set-ups at locations A and B choose a random basis (RNG symbol), rotate the spin accordingly and start the optical spin read-out (measurement symbol). Vertical bars indicate durations. The event-ready signal lies outside the future light cone (coloured regions) of the random basis choices of A and B. **b**, Space–time diagram of the Bell test. The *x* axis denotes the distance along the line AB. The read-out on each side is completed before any light-speed signal can communicate the basis choice from the other side. The uncertainty in the depicted event times and locations is much smaller than the symbol size. **c**, Single-shot spin read-out fidelity at location A as a function of read-out duration (set by the latest time that detection events are taken into account). Blue (orange) line, fidelity of outcome +1 (−1) when the spin is prepared in $m_s = 0$ ($m_s = \pm 1$); green line, average read-out fidelity; dotted line, read-out duration used (3.7 μs). The inset shows the relevant ground and excited-state levels (not to scale).

Before running the Bell test we first characterized the set-up and the preparation of the spin–spin entangled state. Figure 3a displays correlation measurements on the entangled spin-photon states to be used for the entanglement swapping. For both locations A and B we observe near-unity correlations between spin state and photon time bin when spin read-out errors are accounted for. We then estimate the degree of indistinguishability of the single photons emitted at locations A and B in a Hong–Ou–Mandel[31] two-photon-interference experiment at location C, that is, after the photons have travelled through a combined length of 1.7 km of fibre. Using the observed two-photon interference contrast of 0.90 ± 0.06 and the spin-photon correlation data, we estimate that the fidelity to the ideal state ψ^- of the spin–spin entangled states generated in our set-up is 0.92 ± 0.03 (Supplementary Information). Combined with measured read-out fidelities, the generated entangled state is thus expected to violate the CHSH–Bell inequality with $S = 2.30 \pm 0.07$.

As a final characterization we ran the full Bell sequence including random number generation and fast read-out, but with co-linear measurement bases (*ZZ* and *XX*) such that spin–spin correlations could be observed with optimal contrast. To test the fast basis selection and rotation, the Z (X) basis measurements are randomly performed along the $+Z$ ($+X$) and $-Z$ ($-X$) axis. The observed correlations, shown in Fig. 3c (orange bars), are consistent with the estimated quantum state and the independently measured read-out fidelities (dotted bars), which confirms that the set-up is performing as expected and that the desired entangled state is generated.

We find a success probability per entanglement generation attempt of about 6.4×10^{-9}, which yields slightly more than one event-ready signal per hour. Compared to our previous heralded entanglement experiments over 3 m (ref. 29), this probability is reduced, mainly owing to additional photon loss (8 dB km^{-1}) in the 1.7-km optical fibre. To ensure the required long-term operation, we exploit active stabilization on different relevant timescales via automated feedback loops (Supplementary Information). We note that the distance between the entangled electrons is nearly two orders of magnitude larger than it was in any previous experiment[7,10,29,32] with entangled matter systems.

Using the results of the characterization measurements we determine the optimal read-out bases for our Bell test. A numerical optimization yields the following angles for the read-out bases with respect to Z: 0 (for $a = 0$), $+\pi/2$ (for $a = 1$), $-3\pi/4 - \varepsilon$ (for $b = 0$) and $3\pi/4 + \varepsilon$ (for $b = 1$), with $\varepsilon = 0.026\pi$. Adding the small angle ε is beneficial because of the stronger correlations in *ZZ* compared to *XX*. Furthermore, we use the characterization data to determine the time window for valid photon-detection events at location C to optimally reject reflected laser light and detector dark counts. We choose this window conservatively to optimize the entangled-state fidelity at the cost of a reduced data rate. These settings are then fixed and used throughout the actual Bell test. As a final optimization we replaced the photo-detectors at location C with the best set we had available.

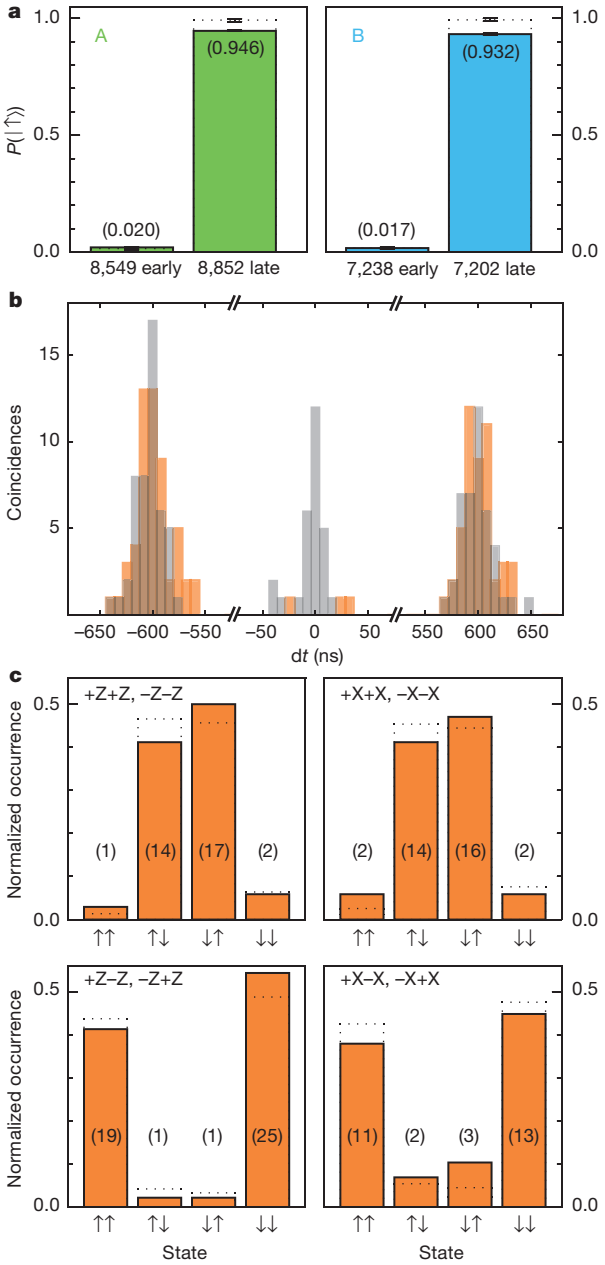

Figure 3 | Characterization of the set-up and the entangled state. **a**, The probability to obtain spin state $|\uparrow\rangle$ at location A (left panel) or B (right panel) when a single photon is detected in the early or late time bin at location C. In the left (right) panel, only emission from A (B) was recorded. Dotted bars are corrected for finite spin read-out fidelity and yield remaining errors of 1.4% ± 0.2% (1.6% ± 0.2%) and 0.8% ± 0.4% (0.7% ± 0.4%) for early and late detection events, respectively, from set-up A (B). These errors include imperfect rejection of the excitation laser pulses, detector dark counts, microwave-pulse errors and off-resonant excitation of the NV. **b**, Two-photon quantum interference signal, with dt the time between the two photo-detection events. When the NV centres at A and B emit indistinguishable photons, coincident detections of two photons, one in each output arm of the beam-splitter at C, are expected to vanish. The observed contrast between the cases of indistinguishable (orange) and distinguishable (grey) photons (3 versus 28 events in the central peak) yields a visibility of (90 ± 6)% (Supplementary Information). **c**, Characterization of the Bell set-up using (anti-)parallel read-out angles. The spins at A (left arrows on the x axis) and B (right arrows on the x axis) are read out along the $\pm Z$ axis (left panels) or the $\pm X$ axis (right panels). The numbers in brackets are the raw number of events. The dotted lines represent the expected correlations on the basis of the characterization measurements presented in **a** and **b** (Supplementary Information). The data yield a strict lower bound[29] on the state fidelity to $|\psi^-\rangle$ of 0.83 ± 0.05. Error bars are 1 s.d.

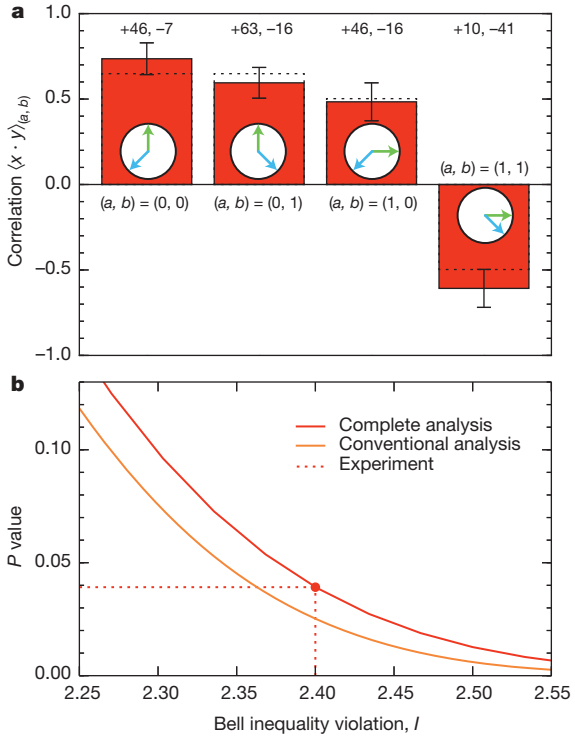

Figure 4 | Loophole-free Bell inequality violation. **a**, Summary of the data and the CHSH correlations. The read-out bases corresponding to the input values are indicated by the green (for A) and blue (for B) arrows. Dotted lines indicate the expected correlation on the basis of the spin read-out fidelities and the characterization measurements presented in Fig. 3 (Supplementary Information). Numbers above the bars represent the number of correlated and anti-correlated outcomes, respectively. Error bars shown are $\sqrt{\left(1-\langle x\cdot y\rangle^2_{(a,b)}\right)/n_{(a,b)}}$, with $n_{(a,b)}$ the number of events with inputs (a, b). **b**, Statistical analysis for $n = 245$ trials. For the null-hypothesis test performed (Supplementary Information), the dependence of the P value on the I value is shown (complete analysis, red). Here $I = 8\left(\frac{k}{n}-\frac{1}{2}\right)$, with k the number of times $(-1)^{(a\cdot b)}x\cdot y = 1$. (For equal $n_{(a,b)}$, $I = S$ with S defined in equation (1).) A small P value indicates strong evidence against the null hypothesis. We find $k = 196$, which results in a rejection of the null hypothesis with a $P \leq 0.039$. For comparison, we also plot the P value for an analysis (conventional analysis, orange) assuming independent and identically distributed (i.i.d.) trials, Gaussian statistics, no memory and perfect random-number generators.

We ran 245 trials of the Bell test during a total measurement time of 220 h over a period of 18 days. Figure 4a summarizes the observed data, from which we find $S = 2.42$, in violation of the CHSH–Bell inequality $S \leq 2$. We quantify the significance of this violation for two different scenarios (see Fig. 4b). First, similar to previous work[4–9], we analyse the data under the assumptions that the Bell trials are independent of each other, that the recorded random input bits have zero predictability and that the outcomes follow a Gaussian distribution. This analysis (which we term 'conventional') yields a standard deviation of 0.20 on S. In this case, the null hypothesis that a local-realist model for space-like separated sites describes our experiment is rejected with a P value of 0.019 (see Supplementary Information).

The assumptions made in the conventional analysis are not justified in a typical Bell experiment. For instance, although the locality conditions outlined earlier are designed to ensure independent operation during a single trial, the boxes can in principle have access to the entire history including results from all previous trials and adjust their output to it[16,21]. Our second analysis (which we term 'complete') allows for arbitrary memory, takes the partial predictability of the random input bits into account and also makes no assumption about the probability distributions underlying the data (see Supplementary Information). In

this case, the null hypothesis that an arbitrary local-realist model of space-like separated sites governs our experiment is rejected with a P value of 0.039 (Fig. 4b). This P value might be further tightened in future experiments.

Our experiment realizes the first Bell test that simultaneously addresses both the detection loophole and the locality loophole. Being free of the experimental loopholes, the set-up tests local-realist theories of nature without introducing extra assumptions such as fair sampling, a limit on (sub-)luminal communication or the absence of memory in the set-up. Our observation of a statistically significant loophole-free Bell inequality violation thus indicates rejection of all local-realist theories that accept that the number generators produce a free random bit in a timely manner and that the outputs are final once recorded in the electronics.

Strictly speaking, no Bell experiment can exclude all conceivable local-realist theories, because it is fundamentally impossible to prove when and where free random input bits and output values came into existence[13]. Even so, our loophole-free Bell test opens the possibility to progressively bound such less-conventional theories: by increasing the distance between A and B (for example, to test theories with increased speed of physical influence); by using different random input bit generators (to test theories with specific free-will agents, for example, humans); or by repositioning the random input bit generators (to test theories where the inputs are already determined earlier, sometimes referred to as 'freedom-of-choice'[9]). In fact, our experiment already enables tests of all models that predict that the random inputs are determined a maximum of 690 ns before we record them (Supplementary Information).

Combining the presented event-ready scheme with higher entangling rates (for example, through the use of optical cavities) provides prospects for the implementation of device-independent quantum key distribution[22] and randomness certification[23,24]. In combination with quantum repeaters, this might enable the realization of large-scale quantum networks that are secured through the very same counter-intuitive concepts that inspired one of the most fundamental scientific debates for 80 years[1,2,25].

Received 19 August; accepted 28 September 2015.
Published online 21 October 2015.

1. Bell, J. S. On the Einstein–Podolsky–Rosen paradox. *Physics* **1,** 195–200 (1964).
2. Einstein, A., Podolsky, B. & Rosen, N. Can quantum-mechanical description of physical reality be considered complete? *Phys. Rev.* **47,** 777–780 (1935).
3. Freedman, S. J. & Clauser, J. F. Experimental test of local hidden-variable theories. *Phys. Rev. Lett.* **28,** 938–941 (1972).
4. Aspect, A., Dalibard, J. & Roger, G. Experimental test of Bell's inequalities using time-varying analyzers. *Phys. Rev. Lett.* **49,** 1804–1807 (1982).
5. Weihs, G., Jennewein, T., Simon, C., Weinfurter, H. & Zeilinger, A. Violation of Bell's inequality under strict Einstein locality conditions. *Phys. Rev. Lett.* **81,** 5039–5043 (1998).
6. Rowe, M. A. *et al.* Experimental violation of a Bell's inequality with efficient detection. *Nature* **409,** 791–794 (2001).
7. Matsukevich, D. N., Maunz, P., Moehring, D. L., Olmschenk, S. & Monroe, C. Bell inequality violation with two remote atomic qubits. *Phys. Rev. Lett.* **100,** 150404 (2008).
8. Ansmann, M. *et al.* Violation of Bell's inequality in Josephson phase qubits. *Nature* **461,** 504–506 (2009).
9. Scheidl, T. *et al.* Violation of local realism with freedom of choice. *Proc. Natl Acad. Sci. USA* **107,** 19708–19713 (2010).
10. Hofmann, J. *et al.* Heralded entanglement between widely separated atoms. *Science* **337,** 72–75 (2012).
11. Giustina, M. *et al.* Bell violation using entangled photons without the fair-sampling assumption. *Nature* **497,** 227–230 (2013).
12. Christensen, B. G. *et al.* Detection-loophole-free test of quantum nonlocality, and applications. *Phys. Rev. Lett.* **111,** 130406 (2013).
13. Brunner, N., Cavalcanti, D., Pironio, S., Scarani, V. & Wehner, S. Bell nonlocality. *Rev. Mod. Phys.* **86,** 419–478 (2014).
14. Garg, A. & Mermin, N. D. Detector inefficiencies in the Einstein-Podolsky-Rosen experiment. *Phys. Rev. D* **35,** 3831–3835 (1987).
15. Eberhard, P. H. Background level and counter efficiencies required for a loophole-free Einstein-Podolsky-Rosen experiment. *Phys. Rev. A* **47,** R747–R750 (1993).
16. Barrett, J., Collins, D., Hardy, L., Kent, A. & Popescu, S. Quantum nonlocality, Bell inequalities, and the memory loophole. *Phys. Rev. A* **66,** 042111 (2002).
17. Bell, J. S. Atomic-cascade photons and quantum-mechanical nonlocality. *Comments Atom. Mol. Phys.* **9,** 121–126 (1980).
18. Żukowski, M., Zeilinger, A., Horne, M. A. & Ekert, A. K. "Event-ready-detectors" Bell experiment via entanglement swapping. *Phys. Rev. Lett.* **71,** 4287–4290 (1993).
19. Simon, C. & Irvine, W. T. M. Robust long-distance entanglement and a loophole-free Bell test with ions and photons. *Phys. Rev. Lett.* **91,** 110405 (2003).
20. Clauser, J. F., Horne, M. A., Shimony, A. & Holt, R. A. Proposed experiment to test local hidden-variable theories. *Phys. Rev. Lett.* **23,** 880–884 (1969).
21. Gill, R. D. Time, finite statistics, and Bell's fifth position. In *Proc. Foundations of Probability and Physics 2* 179–206 (Växjö Univ. Press, 2003).
22. Acín, A. *et al.* Device-independent security of quantum cryptography against collective attacks. *Phys. Rev. Lett.* **98,** 230501 (2007).
23. Colbeck, R. *Quantum and Relativistic Protocols for Secure Multi-Party Computation.* PhD thesis, Univ. Cambridge (2007); http://arxiv.org/abs/0911.3814.
24. Pironio, S. *et al.* Random numbers certified by Bell's theorem. *Nature* **464,** 1021–1024 (2010).
25. Bell, J. S. *Speakable and Unspeakable in Quantum Mechanics: Collected Papers on Quantum Philosophy* 2nd edn (Cambridge Univ. Press, 2004).
26. Gerhardt, I. *et al.* Experimentally faking the violation of Bell's inequalities. *Phys. Rev. Lett.* **107,** 170404 (2011).
27. Robledo, L. *et al.* High-fidelity projective read-out of a solid-state spin quantum register. *Nature* **477,** 574–578 (2011).
28. Barrett, S. D. & Kok, P. Efficient high-fidelity quantum computation using matter qubits and linear optics. *Phys. Rev. A* **71,** 060310 (2005).
29. Bernien, H. *et al.* Heralded entanglement between solid-state qubits separated by three metres. *Nature* **497,** 86–90 (2013).
30. Abellan, C., Amaya, W., Mitrani, D., Pruneri, V. & Mitchell, M. W. Generation of fresh and pure random numbers for loophole-free Bell tests. Preprint available at http://arxiv.org/abs/1506.02712.
31. Hong, C. K., Ou, Z. Y. & Mandel, L. Measurement of subpicosecond time intervals between two photons by interference. *Phys. Rev. Lett.* **59,** 2044–2046 (1987).
32. Ritter, S. *et al.* An elementary quantum network of single atoms in optical cavities. *Nature* **484,** 195–200 (2012).

Supplementary Information is available in the online version of the paper.

Acknowledgements We thank A. Acín, A. Aspect, P. Bierhorst, A. Doherty, R. Gill, P. Grünwald, M. Giustina, L. Mancinska, J. E. Mooij, T. Vidick, H. Weinfurter and Y. Zhang for discussions and/or reading our manuscript, and M. Blauw, P. Dorenbos, R. de Stefano, C. Tiberius, T. Versluis, R. Zwagerman and Facilitair Management and Vastgoed for help with the realization of the laboratories and the optical fibre connections. We acknowledge support from the Dutch Organization for Fundamental Research on Matter (FOM), the Dutch Technology Foundation (STW), the Netherlands Organization for Scientific Research (NWO) through a VENI grant (T.H.T.) and a VIDI grant (S.W.), the Defense Advanced Research Projects Agency QuASAR program, the Spanish MINECO project MAGO (reference FIS2011-23520) and Explora Ciencia (reference FIS2014-62181-EXP), the European Regional Development Fund (FEDER) grant TEC2013-46168-R, Fundacio Privada CELLEX, FET Proactive project QUIC and the European Research Council through projects AQUMET and HYSCORE.

Author Contributions B.H., H.B. and R.H. devised the experiment. B.H., H.B., A.E.D., A.R., M.S.B., J.R., R.F.L.V. and R.N.S. built and characterized the experimental set-up. M.W.M., C.A. and V.P. designed the quantum random-number generators (QRNGs), M.W.M. and C.A. designed the randomness extractors, and W.A. and C.A. built the interface electronics and the QRNG optics, the latter with advice from V.P. C.A. and M.W.M. designed and implemented the QRNG statistical metrology. C.A. designed and implemented the QRNG output tests. M.M. and D.J.T. grew and prepared the diamond device substrates. H.B. and M.S.B. fabricated the devices. B.H., H.B., A.E.D., A.R. and N.K. collected and analysed the data, with support from T.H.T. and R.H. D.E. and S.W. performed the theoretical analysis. B.H., A.R., T.H.T., D.E., S.W. and R.H. wrote the manuscript. R.H. supervised the project.

Author Information Reprints and permissions information is available at www.nature.com/reprints. The authors declare no competing financial interests. Readers are welcome to comment on the online version of the paper. Correspondence and requests for materials should be addressed to R.H. (r.hanson@tudelft.nl).